Fusion Joining of Thermoplastic Composite Wind Turbine Blades: Lap-Shear Bond Characterization

Robynne E. Murray[1], Jason Roadman, Ryan Beach
National Renewable Energy Laboratory, 15013 Denver West Parkway, Golden, CO 80401
[1]robynne.murray@nrel.gov

***Abstract*— Wind turbine blades are typically manufactured from a small number of components which are bonded together with an adhesive. Over the life span of a wind turbine, the static and fatigue loads in varying environmental conditions can lead to cracking and/or debonding of the adhesive joints, ultimately leading to blade structural collapse. The objective of this work is to investigate fusion joining of wind turbine blades manufactured using thermoplastic resin. Thermoplastic resins for wind turbine blades can reduce cycle times and energy consumption during manufacturing and facilitate end-of-life recycling and on-site manufacturing. Additionally, fusion joining of these materials can replace adhesives, resulting in stronger and more robust blades. This work showed that, compared to typical adhesives used in wind turbine blades, fusion welding resulted in an increase in both the static and fatigue lap-shear strength as compared to bonded thermoplastic composite coupons. This initial coupon-scale research suggests that there is potential for developing fusion welding techniques for full-scale wind turbine blades.**

Keywords— Fusion joining; Thermoplastic resin; Lap-shear strength; Composite; Wind turbine blade

1 Introduction

Modern wind turbine blades are commonly manufactured in several key components and bonded together with an adhesive. As shown in Figure 1, high- and low-pressure skins of the blade are bonded together to form the aerodynamic shell. The shear web supports the skins, resists buckling, and transfers shear loads, and the spar caps are the main load-carrying structure along the blade span and are typically manufactured as part of the skins. Over the life span of a wind turbine, blades are exposed to static and cyclic fatigue loads in varying environmental conditions that can cause cracking and/or debonding of the adhesive joints, leading to blade structural collapse [1-4]. For example, Jensen et al. [5] statically loaded a 34-m composite wind turbine blade until failure and found that debonding of the outer skin was the initial failure mechanism, followed by delamination buckling, causing the blade's collapse. Overgaard et al. [6, 7] loaded a 25-m wind turbine blade in static flapwise bending until collapse and asserted that the structural stability was governed by buckling and delamination. Yang et al. [8] characterized a 40 m wind turbine blade under flapwise static loading until collapse and concluded that adhesive debonding between the high-pressure and low-pressure shells was the initial failure mechanism. Further, Zarouchas [9] showed that for an I-beam wind turbine blade subcomponent, according to a finite element simulation, failure began in the elements corresponding to the bond line. Finally,

Pursuant to the DOE Public Access Plan, this document represents the authors' peer-reviewed, accepted manuscript. The published version of the article is available from the relevant publisher.

static loading to failure of a 13-m wind turbine blade designed by Sandia National Laboratories [10] and structurally characterized at the National Wind Technology Center showed significant debonding between the shear web, spar caps, and blade skins, as evident in Figure 1. This outcome highlights the challenges associated with adhesives used in wind turbine blades.

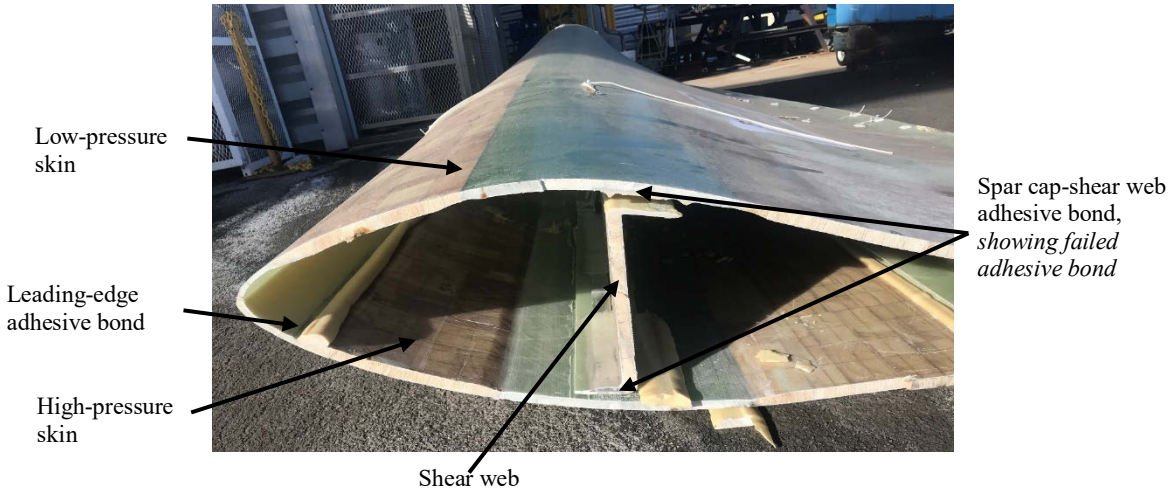

Figure 1 Cross section of Sandia National Laboratories' National Rotor Testbed 13-m blade after planned loading to failure, showing adhesive bond line failures. The photo also shows three key bond lines: high-pressure to low-pressure blade skin bond at the leading edge, and the shear web bonds to both the high- and low-pressure spar caps.

Wind turbine blades are typically constructed of glass and/or carbon fibers and a thermoset resin such as epoxy. However, with the recent development of a two-part acrylic-based reactive thermoplastic resin system, including the successful demonstration of manufacturing a 9-m thermoplastic blade [11], thermoplastic resins have been gaining interest as a replacement for thermosets in wind turbine blades because of their room temperature cure, recyclability [12], and decreased cycle times, which could lead to lower manufacturing costs [13-16]. Another advantage of thermoplastic composites is the potential for fusion welding, which could eliminate the need for adhesive bonds between blade components and increase the overall strength and reliability of the blades. Fusion bonding takes advantage of the property of thermoplastic matrices to flow when heated above their glass transition temperature and then return to their baseline mechanical properties upon cooling down [17]. The glass transition temperature is the temperature range in which a material changes from a hard state to a more pliable, compliant state. This facilitates the joining of two parts by fusing their contacting surfaces when heated. Subsequent cooling of the bond under pressure results in the polymeric chains entangling to form a strong bond.

The use of adhesives to bond wind turbine blades is also a time-consuming in-mold process during blade manufacturing, taking approximately 30 minutes for paste application and 3–4 hours for the curing cycle [18]. This affects the blade cycle time and ultimately costs the manufacturer, therefore, replacing adhesives with fusion welding has the potential to reduce the in-mold cycle time in the manufacturing facilities as well as the wind turbine blade costs. Because infusible thermoplastic resins are in the

Pursuant to the DOE Public Access Plan, this document represents the authors' peer-reviewed, accepted manuscript. The published version of the article is available from the relevant publisher.

early stage of development, fusion joining of wind turbine blades using thermoplastic resins is a new field of study. The objective of this work is to investigate and demonstrate fusion joining processes for infusible thermoplastic resins and determine the feasibility of replacing adhesives with this new joining method for wind turbine blades.

Fusion joining has been investigated thoroughly for thermoplastic materials [17, 19-23]; however, previous research focused on applications such as aerospace, which use higher cure-temperature materials and manufacturing processes that are not viable for large wind turbine blades [24]. Arkema Inc has developed a new thermoplastic resin that has a lower glass transition temperature, making this process more feasible for wind turbine blades. Fusion joining of a thermoplastic wind turbine blade can be done by focusing heat and pressure at the location of a joint within the blade, enabling localized heating to fuse the two contacting surfaces without heating the entire blade, which could cause it to lose its shape or produce fiber disturbances in the laminates. There are several methods by which to apply heat to a joint, including, but not limited to, mechanical motion resulting in friction melting, electric-resistance heating, ultrasonic, microwave, and induction heating [25, 26]. Of the fusion bonding methods, ultrasonic, resistance, and induction welding have been widely researched for other applications [17, 19-21, 24, 27, 28].

The challenges of fusion joining for wind turbine blades arise from the need to use relatively low-cost methods that result in reliable and strong bonds with minimal additional floor space and equipment requirements in the manufacturing facility. In addition, the method used must be compatible with current blade manufacturing technology and tooling or require a change in manufacturing that results in a lower final blade cost. These challenges limit the joining methods that can be used. For example, friction welding is not perceived to be a suitable solution for the wind industry because of the requirements to physically move the joining surfaces, which would not be possible with current blade tooling. The authors think that resistance and induction welding show the most promise for wind turbine blade joining and are the focus of these initial investigations.

Induction welding uses a high-powered coil with an alternating voltage to produce a magnetic field in an electrically conductive and possibly magnetically susceptible implant (heating element or susceptor) between adherend interfaces. The magnetic field stimulates eddy currents and heats the implant. The eddy currents are resisted by the heating element material that results in energy losses and heat production. To weld materials using induction heating, the susceptor is heated, in conjunction with the application of pressure to consolidate the materials. A schematic of this method is shown in Figure 2 (left). Ahmed [17] provides a more in-depth description of the induction welding process including heating mechanisms and parameters that govern the welding process.

Induction welding requires no contact between the induction coil and the heating element and can be designed such that only the interface materials are affected by the magnetic field, hence no heat is produced outside of the desired weld area. This results in a low-energy consumption process because only the susceptor and interface materials heat up. However, one of the

Pursuant to the DOE Public Access Plan, this document represents the authors' peer-reviewed, accepted manuscript. The published version of the article is available from the relevant publisher.

challenges with induction heating is the sensitivity to the working distance between the heating element and the coil, and the ability of the magnetic field to couple to heating element materials that are feasible for use in a wind turbine blade. For wind blades, the thickness of the laminates through which the susceptor needs to be heated changes over the blade length due to ply drops in the spar cap; therefore, accurately controlling the coil distance will be important. For induction welding of wind turbine blades, it is also important to consider the materials used in both the tooling and the blade itself. For consideration, if there is carbon-fiber material in the blade other than at the bond lines, or metal material in the tooling frames, careful consideration has to be given to the system design to avoid unwanted heating. Furthermore, temperature uniformity in the heating element plays an important role in the bond quality and can be challenging because of edge effects in the heating element. To enable better control of the bonding temperature, "smart" susceptor materials can be used such that the Curie point (the temperature at which a magnetic material becomes nonmagnetic) is just above the glass transition temperature of the resin [24, 29]. This can result in levelling of the susceptor temperature independent of the applied power (temperature plateaus at a predetermined point). This method has been employed by Boeing [24] to control the peak temperatures during the consolidation stage of manufacturing higher-temperature thermoplastic aerospace components. It is a challenge to find a magnetic material with a Curie point compatible with the lower-glass transition temperature thermoplastic resin that can be used in a wind turbine blade.

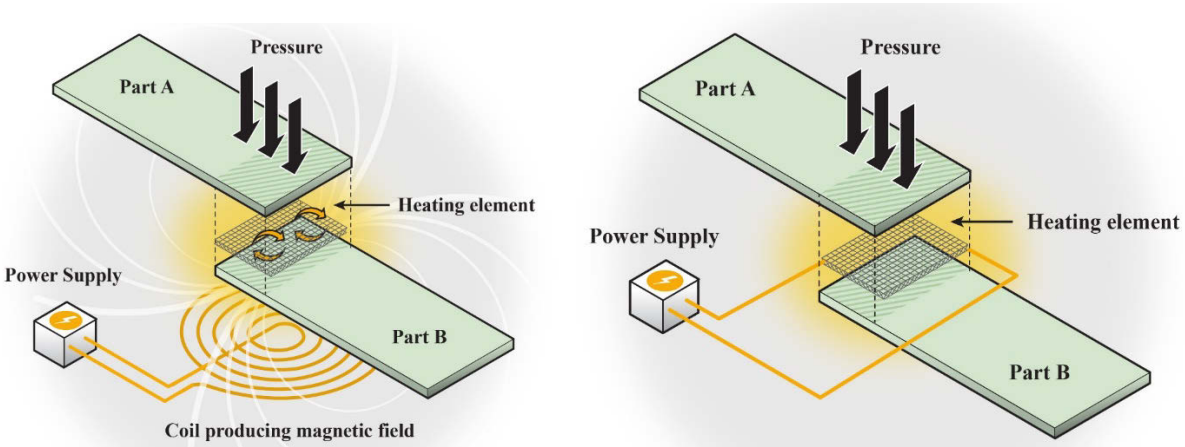

Figure 2 Schematic of induction welding (left) and resistance welding (right), with a heating element embedded between two composite adherends.

Resistance welding of thermoplastic components involves applying a current to heat an electrically conducting heating element implanted between two adherend surfaces, with pressure applied for consolidation. This is typically done by sandwiching a conductive material, such as a metal mesh or carbon fiber, between two components with a connection to a power source, as shown in Figure 2 (right). When current flows through the heating element, the heat generated follows Joule's Law, wherein the energy dissipated is proportional to the resistance, current, and elapsed time [21]. The benefits of resistance welding include low-cost equipment and easy operation, mainly attributed to the relatively simple relationship between the current and heat. However,

Pursuant to the DOE Public Access Plan, this document represents the authors' peer-reviewed, accepted manuscript. The published version of the article is available from the relevant publisher.

this method may be difficult to scale up because of power and voltage requirements for longer bond lines. Welding smaller sections sequentially has been demonstrated to be viable for welding large-scale joints under realistic power levels and pressures; however, temperature nonuniformity in the welding area and current leaking to the laminate (when carbon-fiber adherends are used) have been shown to be issues with scaled-up weld areas [20]. In addition, resistance welding requires physical contact with the welded joint, which could pose challenges to connect the heating element to the power supply for the internal joints on a wind turbine blade. Furthermore, this method requires a continuous loop for the conductive material, which will have to be considered in the design of the lightning protection systems in wind turbine blades. However, continuous carbon fiber is currently used in some wind turbine blade spar caps; therefore, using it as the heating element material may help reduce these concerns. For both induction and resistance welding, the fact that the heating element remains in the weld opens the possibility of reprocessing if there is incomplete bonding or damage to the blade in the field.

2 Materials and Methods

The bond lines in wind turbine blades fail because of initiation and propagation of cracks in the adhesives. From fracture mechanics, there are three ways to load a joint to cause a crack to propagate and ultimately fail. A Mode I fracture results from a tensile load normal to the crack (peel), a Mode II fracture is a sliding mode that results from an in-plane shear stress, and a Mode III fracture is a tearing mode that results from an out-of-plane shear. Mode I failures can be characterized by peel tests or double cantilever beam tests, depending on the compliance of the bond, whereas Mode II failures are often characterized by lap-shear tests, (although there are additional bending loads due to load eccentricity in lap shear tests which means there are also some Mode I loading, especially contributing to crack initiation. Wind turbine blade bond lines are subjected to mixed-mode loading conditions, resulting in a combination of Mode I and Mode II failures [30], with the type of failure varying depending on where the bond is located in the blade [31, 32]. Although wind turbine blade bond lines are subjected to mixed mode failures, lap-shear characterization is the focus for this initial work. Further Mode I characterization is planned for the future.

Pursuant to the DOE Public Access Plan, this document represents the authors' peer-reviewed, accepted manuscript. The published version of the article is available from the relevant publisher.

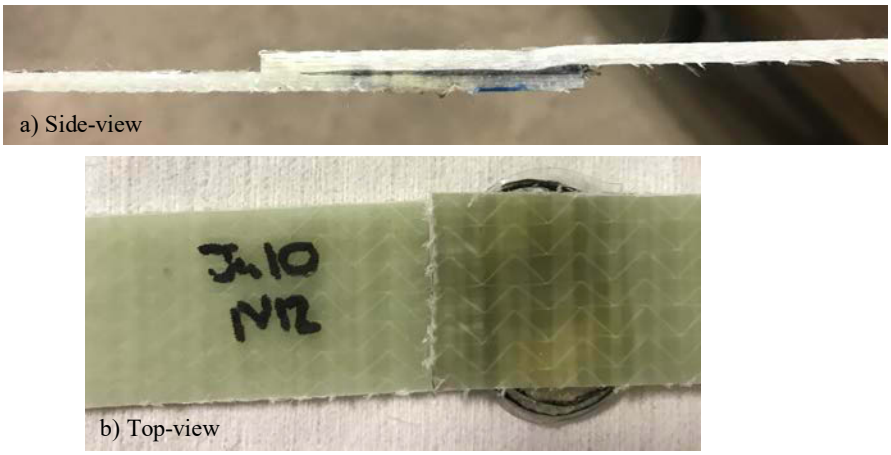

Figure 3 Image of fusion joined thermoplastic composite adherends with embedded carbon fiber heating element, a) side-view, b) top-view

2.1 Characterization methodology

Lap-shear characterization following the ASTM D5868 standard using resistance- and induction-welded joints, as well as adhesive bonded joints, was used to investigate the feasibility of advanced joining methods prior to scaling up to blade-scale. A 100-kN MTS load frame was used to perform both static and fatigue lap-shear characterization. The static experiments were loaded at a rate of 13 mm/min, as per the ASTM standard, and the fatigue experiments were carried out under ambient laboratory conditions at a frequency of 10 Hz and a stress ratio of R=0.1. This R-ratio was chosen based on previous tests done using adhesives. The temperature of the specimens was monitored during each experiment using an infrared camera and a maximum temperature rise of 4°C was observed over all tests. This temperature rise demonstrates that the chosen frequency is acceptable based on ASTM standards for fatigue testing, which suggests a maximum temperature rise of 10°C. A specimen was deemed to have failed when a bond pulled apart completely or the specimen lost over 20% of its initial strength. If a specimen did not fail, the experiment was terminated at 10 million cycles. To minimize bending loads in the joints during both static and fatigue characterization, end tabs of the same thickness as the adherends were used. A grip pressure of 800 PSI (5.52 MPa) was used for all experiments.

2.2 Bonding methodology

The adherends used for the lap-shear characterization were cut from panels manufactured using vacuum-assisted resin transfer molding with four layers of Johns Manville 086 unidirectional fiberglass (1200 g/m^2 fabric with sizing appropriate for acrylic thermoplastic resin), with acrylic-based Elium-188 thermoplastic resin and 2% peroxide initiator by weight. The final

Pursuant to the DOE Public Access Plan, this document represents the authors' peer-reviewed, accepted manuscript. The published version of the article is available from the relevant publisher.

composite panel had 25% resin by volume. The adherends were 101.6 mm long, 25.4 mm wide, and 3.5 mm thick, and were bonded with a 645-mm^2 bonding area, as per the ASTM standard, (shown in Figure 2). The same thermoplastic fiberglass composite adherends were used for both the adhesive and the fusion-welded bonds. All bonding surfaces were roughened with 180 grit sand paper and wiped clean with a clean dry cloth prior to bonding.

For fusion bonding, the coupons were placed into a ceramic fixture and pressure was applied via a ceramic block on the top of the bond using a PHASE IIAFG-0600 force gauge to hold and measure pressure. For both resistance and induction welding, a combination of embedded Omega model TT-K-40-100 thermocouples (0.0799-mm diameter) and a FLIR infrared camera were used to monitor the bond line temperatures. An EtherCAT data acquisition system based on National Instrument's EtherCAT PXI technology combined with National-Renewable-Energy-Laboratory-developed LabVIEW coded software was used to log the temperature, current, and voltage data at 100 Hz. The pressure, weld time, and temperature were optimized based on the lap-shear strength. For all welding methods and heating elements used, a pressure of 50 PSI (0.345 MPa) resulted in sufficient consolidation of the joint without compressing the fibers or squeezing out too much excess resin. Consolidation was verified by investigating the adherend surface above the weld using an OmniScan MX2 phased array ultrasonic scanner with a 16-element probe operating at a frequency of 5 MHz to ensure that the adherend coupon did not have any delamination. A bond interface temperature of 200°C was found to produce the highest strength bonds. The Elium resin has a glass transition temperature of approximately 110°C; however, it was necessary to heat above this to achieve enough resin flow. The heating time varied between 5 and 10 minutes, depending on the heating element used and the time required to reach the desired bond temperature. Following the determination of the optimized input parameters, five repeat lap-shear specimens were made for each heating element and welding method combination.

2.2.1 Heating elements

Several different heating element materials were investigated for both resistance and induction welding. The resistance of the heating element is one of the most important parameters in the welding process because it dictates the required power input. Therefore, several heating element options were eliminated because of poor electrical conductivity, leading to unobtainable power requirements. For example, a carbon-fiber veil was trialled as a heating element for resistance welding; however, because of the shorter and more randomly oriented fiber strands, the power input required to heat the veil surpassed the input capabilities of the power supply used. Furthermore, the veil fabric easily broke apart when the connection to the power supply was applied. It was found that small-diameter stainless-steel mesh and plain-weave carbon-fiber and unidirectional carbon-fiber heating elements were able to be heated with a reasonable amount of power input. The heating elements were preinfused with the thermoplastic resin using vacuum-assisted resin transfer molding with rubber surrounding the fibers on the outside edges to shield them from

Pursuant to the DOE Public Access Plan, this document represents the authors' peer-reviewed, accepted manuscript. The published version of the article is available from the relevant publisher.

resin saturation. The rubber was removed after infusion, which provided dry fibers to connect the power supply to. For all heating elements, an addition of a 0.2-mm-thick layer of acrylic neat resin film on either side of the heating elements was used to ensure enough resin at the bond line. Table 1 summarizes the joining methods and materials investigated in this work. The following sections outline these processes in more detail. Results of the lap-shear characterizations are given in Section 4.

Table 1 Summary of bonds characterized including materials and heating method

Bond method	*Materials*	*Bond preparation*
Adhesive bonds	Acralock SA10-60 epoxy-based adhesive	A bead of adhesive was applied, along with 1% by weight glass beads, and cured at room temperature under clamp pressure for 48 hours
	Plexus 590 acrylic-based adhesive	
	Plexus 310 acrylic-based adhesive	
Resistance welded-bonds	Stainless-steel 304 mesh with a wire diameter of 0.094 mm and 53% opening area heating element with acrylic film on either side (from McMaster Carr)	A current of 16 A and voltage of 2.5 V was applied to the heating element for 5 minutes
	Fiberglast 4.0-oz unidirectional carbon-fiber heating element infused with Elium 188; multipurpose polyester and epoxy sizing on fibers	A current of 7 A and voltage of 7 V was applied to the heating element for 5 minutes
	Fiberglast 3.5-oz plain-weave carbon-fiber heating element infused with Elium 188; multipurpose polyester and epoxy sizing on fibers	A current of 5.5 A and voltage of 7 V was applied to the heating element for 5 minutes
	Vectorply C-BX 0450 biaxial carbon-fiber heating element infused with Elium 188; 50C sizing on fibers	A current of 6 A and voltage of 4.5 V was applied to the heating element for 10 minutes
Induction-welded bonds	Fiberglast 3.5-oz plain-weave carbon-fiber heating element infused with Elium 188; multipurpose polyester and epoxy sizing on fibers	The induction coil was located 10 mm above the heating element and operated at 4.25 kW (85% of maximum power) for 5 minutes

Figure 4 shows the temperature profiles of various heating elements. These images are meant to demonstrate the temperature uniformity and do not reflect the actual heating element temperature used in the welding process because they were taken without the adherend coupons on either side of the heating element, which normally acts as a heat sink.

Pursuant to the DOE Public Access Plan, this document represents the authors' peer-reviewed, accepted manuscript. The published version of the article is available from the relevant publisher.

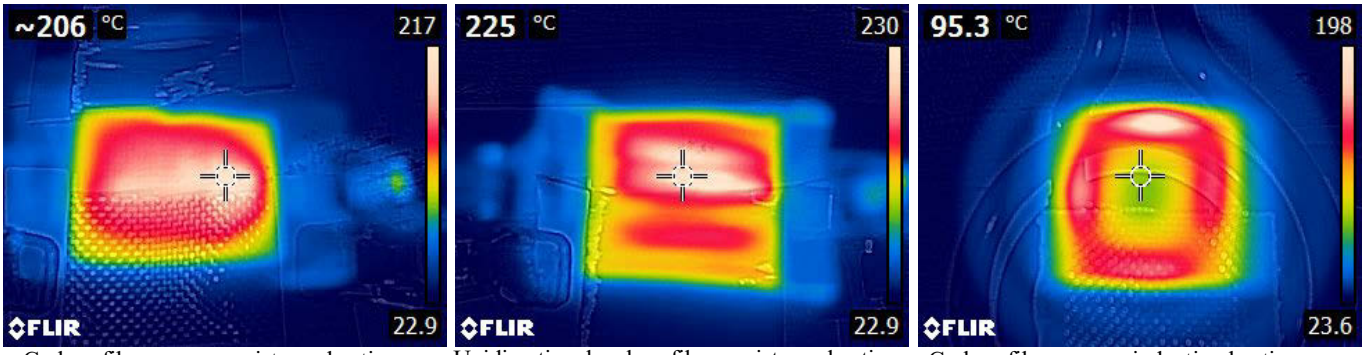

Carbon-fiber weave, resistance heating | Unidirectional carbon-fiber, resistance heating | Carbon-fiber weave, induction heating

Figure 4 Infrared thermal image of (left) resistance-heated carbon-fiber weave, resistance heating of unidirectional carbon fiber (middle), and a metal mesh induction heating element placed 3.5 mm above the top surface of the induction coil (right).

The temperature uniformity of the heating element and bond interface have a strong impact on the strength of a fusion-welded bond. The temperature uniformity of the resistance-welded bonds is dependent on both the heating element fiber pattern and the connection to the power supply. The plain-weave carbon fiber has a more uniform temperature gradient than the unidirectional carbon fiber, as evident in Figure 4 (left). This is a result of the transverse fibers helping to conduct heat and current to the outer edges of the heating element. With induction welding, producing uniform heating in the heating element poses a significant challenge. Because of the small size of the heating element (645-mm^2 area), current buildup around the edges results in significantly higher temperatures at the edges than in the center. As shown in Figure 4 (right), there is more than 100°C difference from the center of the heating element to the outside edges. This temperature nonuniformity was addressed by using lower power for a longer period and insulating around the bond area to help promote more even heating. However, it was not possible to achieve a totally uniform heating element temperature, which is expected to continue to be an issue at a larger scale.

2.2.2 Adhesive bonds

Lap-shear specimens were bonded in accordance with ASTM D5868 using several Methacrylate-based adhesives commonly used in the wind industry: Acralock SA10-60, Plexus 590, and Plexus 310. These adhesive data provide a baseline for comparing the strength of the fusion-welded bonds for wind turbine blades. The bond gaps were controlled with glass beads to a thickness of 0.76 mm, as specified by the ASTM standard. To do this, a small quantity of the glass beads (1% by weight) was applied with the adhesive, as done by [33]. The bonds cured at room temperature under clamp pressure for a minimum of 48 hours in the laboratory. Five specimens were made for each adhesive type.

2.2.3 Resistance bonds

A Versatile Power BENCH 30-33XR 30V/33A programmable power supply was used to apply current across the heating element. The ends of the heating element were clamped via alligator clips between two copper electrodes to make the connection

Pursuant to the DOE Public Access Plan, this document represents the authors' peer-reviewed, accepted manuscript. The published version of the article is available from the relevant publisher.

with the power supply. The setup for resistance welding is shown in Figure 5. One of the challenges with resistance welding of the thermoplastic composite adherends was static buildup on the surface of the nonconductive adherends. To mitigate this static buildup affecting the power supply, the coupons were grounded. Static buildup will be important to consider as bonding is scaled up. In addition, as the heating element was heated, the resistance decreased, hence, the required voltage to obtain the same current decreased as well. Therefore, it is important to have appropriate control of the current to compensate for the changing resistance. In this case, the power input was controlled manually as the resistance changed.

2.2.4 Induction bonds

An SM5 5-kW UltraFlex Power induction heating unit with a three-turn pancake coil with an outer diameter of 65 mm was set up for transverse flux heating of an embedded heating element. A glass rod attached to the load fixture was used to apply pressure to the bond through the coil. The setup for induction welding is shown in Figure 5. A frequency of 157 kHz, power of 4.25 kW (85% of maximum power), and maximum working distance of 10 mm between the coil and heating element were used. The coil was water cooled using an external 25 L capacity chiller. It was found that the induced current in the unidirectional carbon fiber was not sufficient to obtain the temperature rise required for bonding, hence, no induction-welded bonds were made with the unidirectional carbon-fiber heating elements. The greatest challenge with the induction welding was obtaining suitable coupling between the coil and the heating element. To adequately heat the heating element to the required bonding temperature, the coil could be no further than 10 mm above the heating element, for all heating element types. This requirement for a small distance between the coil and the bond area will pose issues for heating through thicker wind turbine blade components such as spar caps that are typically thicker than 10 mm.

a) Resistance welding setup b) Induction welding setup

Pursuant to the DOE Public Access Plan, this document represents the authors' peer-reviewed, accepted manuscript. The published version of the article is available from the relevant publisher.

Figure 5 Image a) showed the resistance welding setup with the connections to the heating element, and pressure application shown, and image b) shows the induction welding setup with the induction coil, induction power supply, and method for pressure application(b. These setups were used to make the specimens for lap-shear characterization.

3 Results and discussion

3.1 Static results

Figure 6 shows the average lap-shear strength of five specimens for various bond types. The error bars indicate the standard deviation for each set of bonds characterized.

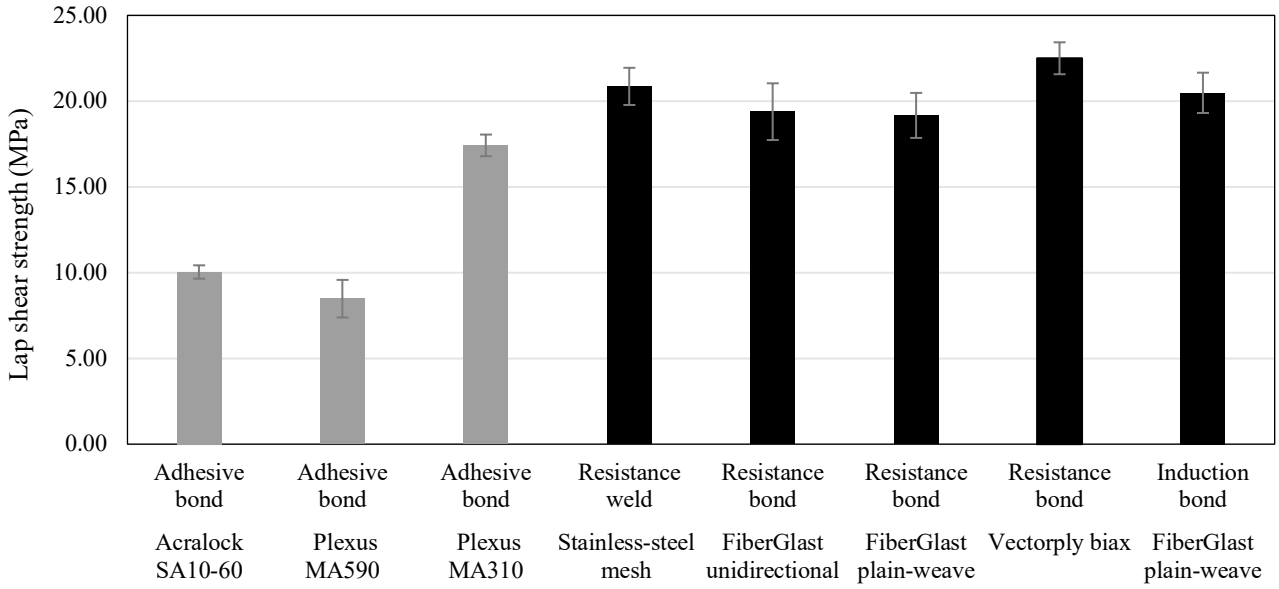

Figure 6 Lap-shear strength of various bond types.

In Figure 6, the resistance- and induction-welded bonds have higher lap-shear strengths than the adhesive bonds by up to 100%. There are three main macroscopic failure modes for adhesives and welded bonds [34-36]. Adhesive/adherent interface failure (interfacial failure) is characterized by the failure between the adhesive and the adherent surface and is one of the lowest shear strength failures, as it indicates that the adhesive was not bonded well to the adherends. Cohesive failure is characterized by the failure within the adhesive, typically through its thickness. This type of failure suggests that the bond between the adherends and the adhesive is stronger than the adhesive strength itself. Finally, adherent failure (coupon failure) is characterized by the failure of the adherent, which indicates that the adhesive is stronger than the adherents and therefore typically comes with high-strength bonds. The type of macroscopic failure mode is identified by observing the adherend fracture surfaces. Examples of the fracture surfaces of the adhesive bonds and fusion bonds are shown in Figure 7.

Pursuant to the DOE Public Access Plan, this document represents the authors' peer-reviewed, accepted manuscript. The published version of the article is available from the relevant publisher.

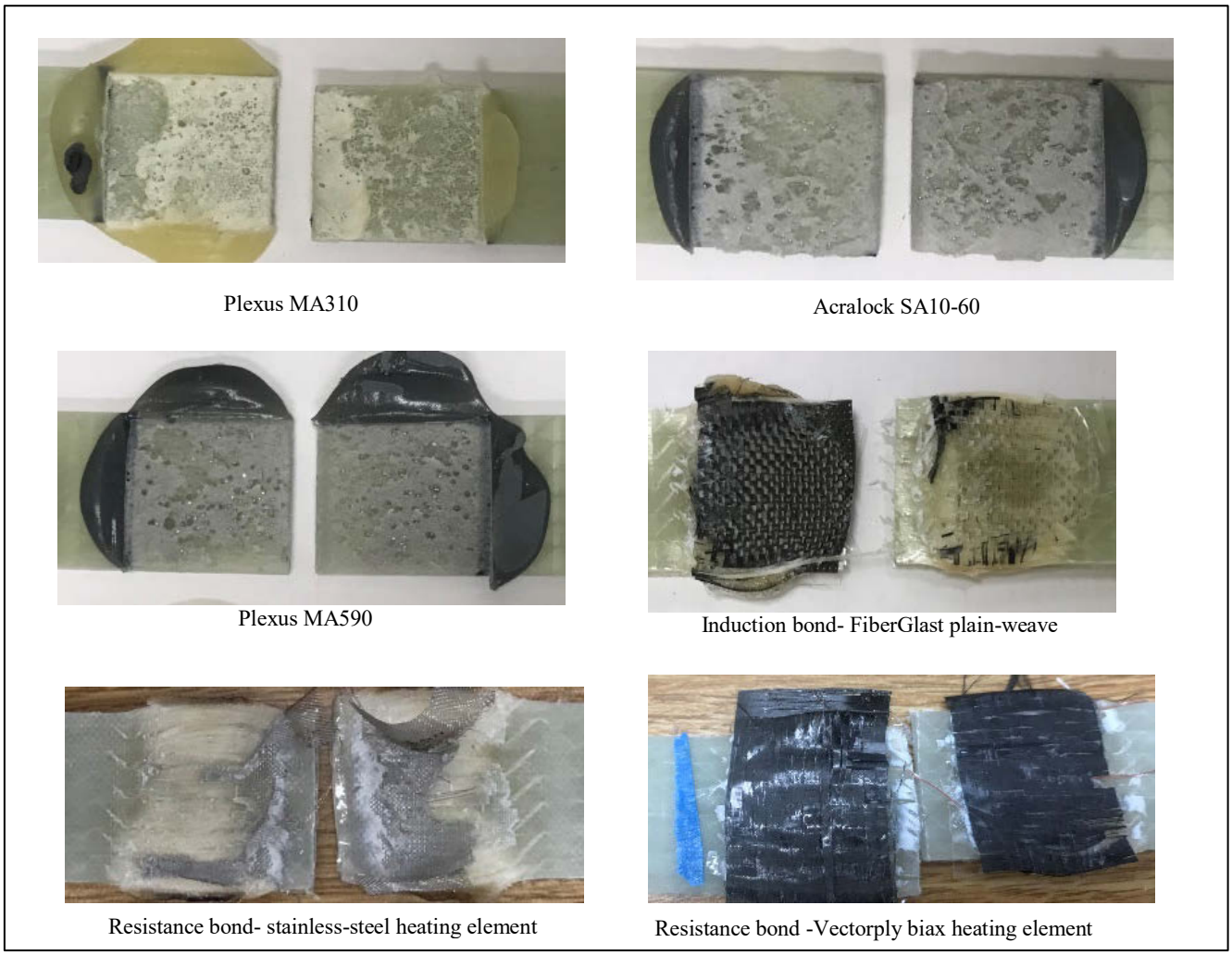

Figure 7 Bond fracture surfaces for adhesive bonds and resistance- and induction-welded bonds.

All three adhesives failed cohesively, which means that the adhesive bonded well to the thermoplastic composite adherends but failed in shear through the thickness. The average lap-shear strength for the Plexus MA310 adhesive was 17.4 MPa, making it the strongest of all three adhesives trialled. However, from the manufacturer, the MA310 adhesive is only intended for use in a bond gap up to 1 mm thick, which would not be suitable for a wind turbine blade in which the bond gap can be up to 20 mm thick. The Acralock and Plexus MA590 had lap-shear strengths of less than 10 MPa, which is low relative to the quoted lap-shear strength from the manufacturer's technical data sheet for bonding epoxy-based fiberglass components [37, 38], but is still within the specifications for wind turbine blades given by DNV-GL [39].

The resistance-welded bonds using the stainless-steel heating element had an average lap-shear strength of 20.9 MPa. The strongest of the stainless-steel bonds failed in a combination of adhesive and cohesive failure in the stainless-steel mesh (the heating element pulled off the coupon in some areas, and broke apart in others), as shown in Figure 7. Although the resin-to-resin bonds in the open area of the mesh were strong, the stainless-steel mesh introduced stress concentrations and residual stresses

Pursuant to the DOE Public Access Plan, this document represents the authors' peer-reviewed, accepted manuscript. The published version of the article is available from the relevant publisher.

because of differences in thermal expansion, acting as a site for cracks to initiate and leading to failure. A similar outcome was found by Ahmed [17]. These stress concentrations caused by the wires are expected to limit the strength of fusion-welded bonds and is another reason for using carbon fiber as a heating element for bonding larger wind turbine blades.

For induction welding, the position of the coil had a significant impact on the bond strength and even slight millimeter-scale changes in the setup between bonds had up to a 10 MPa difference in the lap-shear strengths. This means that when it comes to bonding a large blade, the location of the coil relative to the bond line must be controlled very tightly, which may be challenging given that 1-or 2-mm variations in the laminate thickness will affect the weld quality, and current blade bond line tolerances can be as high as ±10 mm.

The lap-shear strength for the fusion-welded bonds made using carbon-fiber heating elements varied depending on the type of carbon fiber used. The resistance- and induction-welded bonds made with the FiberGlast carbon fiber failed at an average of 19.7 MPa, whereas the bonds with Vectorply biaxial carbon-fiber heating elements failed at an average of 22.5 MPa lap-shear strength. To further explore the failure of the carbon-fiber heating element bonds, a FEI Nova 630 scanning electron microscopy (SEM) was used to look at the fracture surfaces. This tool is a high-resolution Field Emission SEM tool, with a resolution of about 5nm, and the samples were prepared by cutting and imaged with low energy and low current to avoid coating with gold or carbon, unless absolutely necessary. The energy and current settings were adjusted during imaging to alleviate any charging and image artefacts. Figure 8 shows the fracture surface of one side of a failed bond made with the FiberGlast carbon-fiber plain-weave heating element (the side with the carbon fiber remaining, from Figure 7).

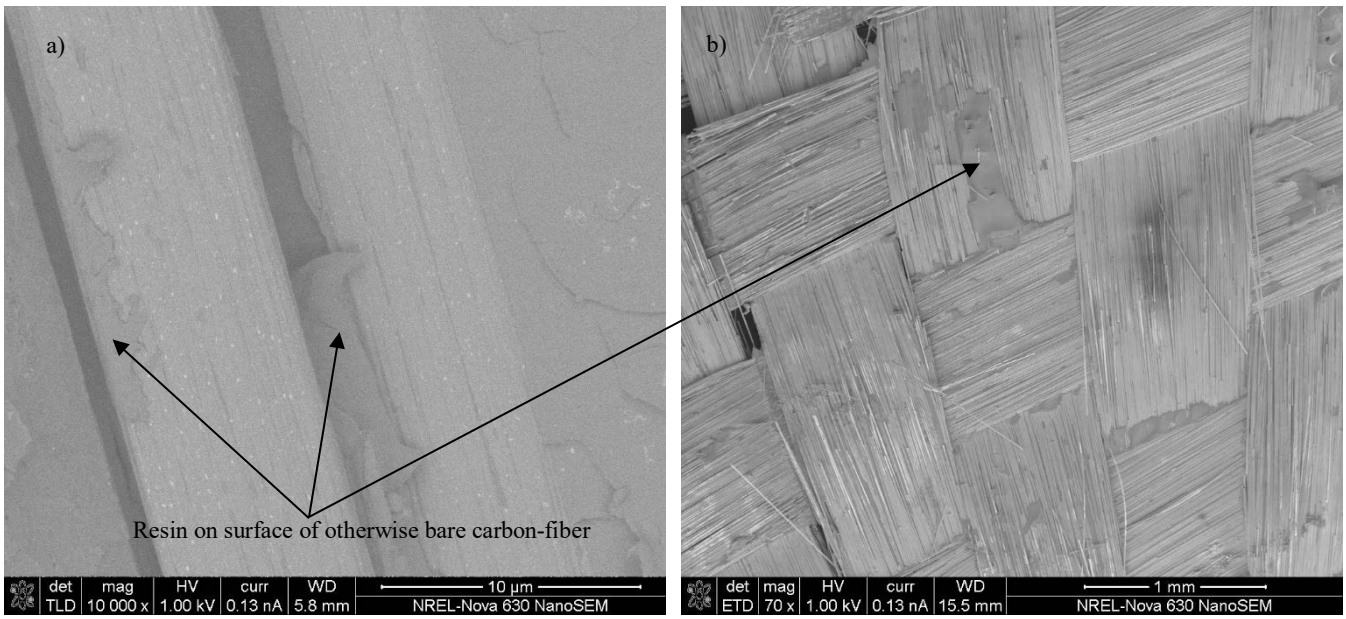

Figure 8 SEM image at two magnification levels (image a showing 10,000 times magnification, and image b showing 70 times magnification) showing the fracture surface of an induction-welded bond made with the FiberGlast carbon-fiber heating element. Area shown is the side with the carbon fiber remaining from Figure 7.

Pursuant to the DOE Public Access Plan, this document represents the authors' peer-reviewed, accepted manuscript. The published version of the article is available from the relevant publisher.

As shown in Figure 8, the thermoplastic resin did not adhere well to the carbon fiber during loading. The resin in the carbon-fiber heating element formed a better bond with the thermoplastic resin in the opposing adherend, leading to the resin pulling apart from the carbon fiber during loading and leaving bare carbon fibers on the heating element surface. There are several possible explanations for this poor resin-to-fiber bonding. An initial theory for the poor resin-fiber bonding of the FiberGlast carbon-fiber bonds was that the carbon-fiber sizing could have been thermally degraded. However, based on literature studies regarding the thermal degradation of fiber sizing [40-42], sizing degradation is not expected to occur after only 5 minutes of heating at the 200°C welding process used here. It was also considered that the carbon-fiber heating element was not fully wet-out during infusion, hence, the resin was only coating the surface and was easily pulled away from the carbon fibers. Figure 9 shows a cross-sectional view of an infused FiberGlast carbon-fiber heating element, prior to being used in a bond. It should be noted that there was damage introduced in the cross-sectional SEM images because of the required cutting and preparation of the samples; however, it is still possible to make observations about how well the heating elements are infused with resin.

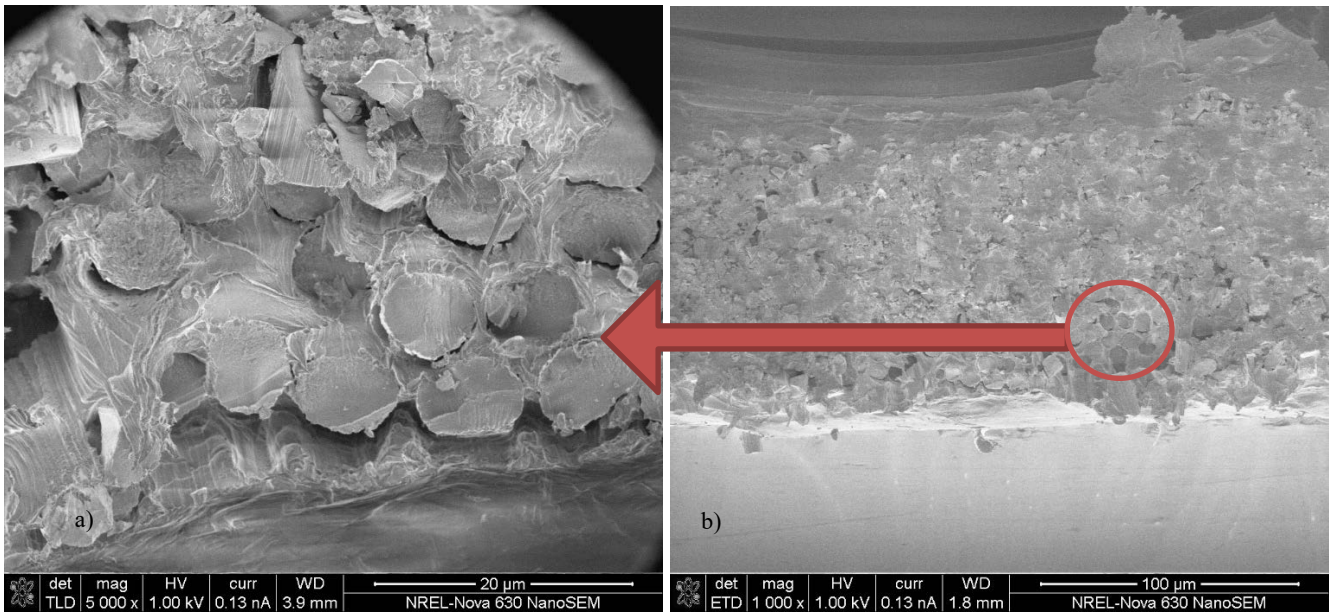

Figure 9 SEM image showing a cross section of infused FiberGlast plain-weave carbon-fiber heating element, at two magnification levels (image a showing 5,000 times magnification, and image b showing 1,000 times magnification).

As shown in Figure 9, the carbon fibers appeared to be fully saturated with resin. Therefore, the poor adhesion of the resin to the fibers is attributed to an incompatibility of the sizing on the carbon fibers with the thermoplastic resin. The FiberGlast unidirectional and plain-woven carbon-fiber fabrics shown in Figure 6 and Figure 7 had a multipurpose fiber sizing that was recommended for use with both epoxy and vinyl-ester resins, and hence was not optimized for one specific resin. Therefore, it is not surprising that the carbon fibers did not adhere well to the thermoplastic resin. Previous work by Arkema Inc has shown the importance of using the correct fiber sizing to achieve a successful bond between the thermoplastic resin and the fibers [43].

Pursuant to the DOE Public Access Plan, this document represents the authors' peer-reviewed, accepted manuscript. The published version of the article is available from the relevant publisher.

The Vectorply biaxial carbon-fiber bonds had good adhesion between the outer layer of carbon fiber and the adherend, but failed between the 0° and 90° carbon fibers, as shown in Figure 7. Figure 10 shows SEM imaging of the cross section of an infused Vectorply biaxial carbon-fiber heating element, prior to being used in a bond.

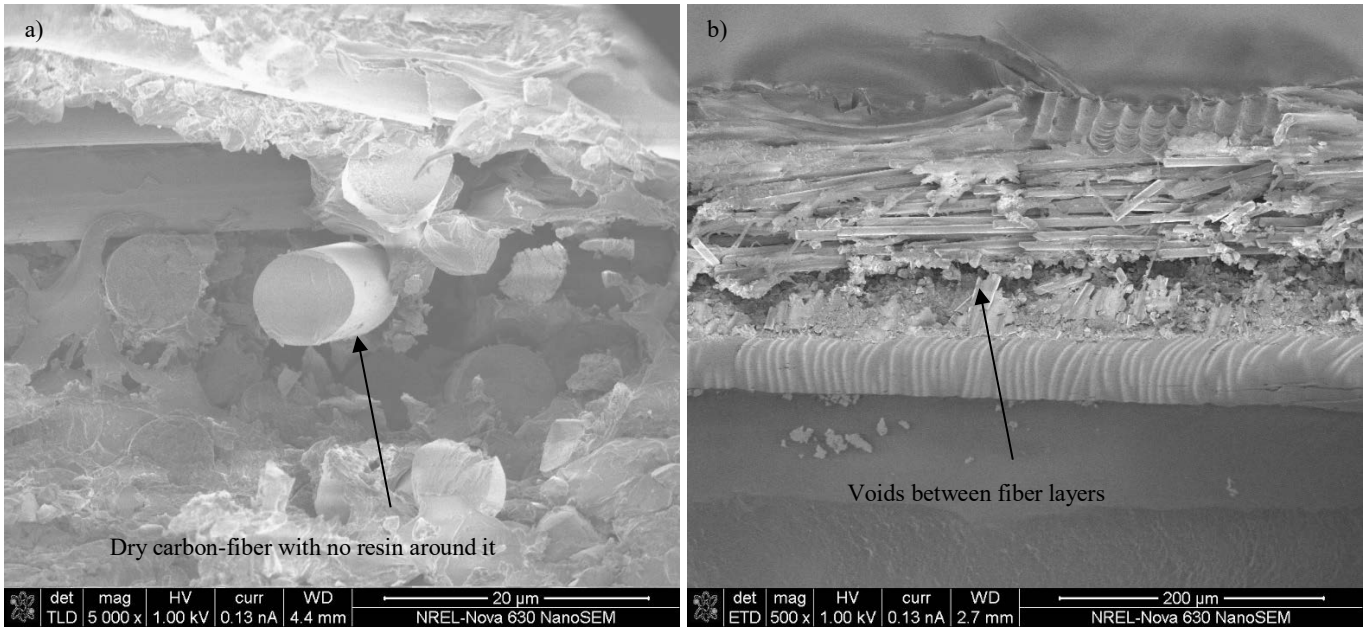

Figure 10 SEM ex situ fractograph showing a cross section of infused Vectorply biaxial carbon-fiber heating element, at two magnification levels (image a showing 5,000 times magnification, and image b showing 500 times magnification).

The SEM imaging of the biaxial heating element (Figure 10) showed that there were voids and dry fibers in the interface between the 0° and 90° carbon fibers, which suggests that the heating elements were not fully infused prior to fusion welding. This likely led to failure initiating at this location. The Vectorply biaxial fabric with the 50°C sizing was selected based on a suggestion from the resin manufacturer and is expected to be more compatible with the thermoplastic resin. However, it is not clear if the sizing could have also contributed to failure between the carbon-fiber layers. Future work is needed to further explore the effects of sizing and investigate improved infusion methods to ensure full wet-out of the heating elements.

Another important characteristic of bond quality is ductility. Ductility is the ability of the bond to deform or elongate under loading and is defined as the displacement of the bond during lap-shear characterization divided by the original bond length (25.4 mm this case). The lap-shear stress as a function of percent elongation for four bond types are shown in Figure 11.

Pursuant to the DOE Public Access Plan, this document represents the authors' peer-reviewed, accepted manuscript. The published version of the article is available from the relevant publisher.

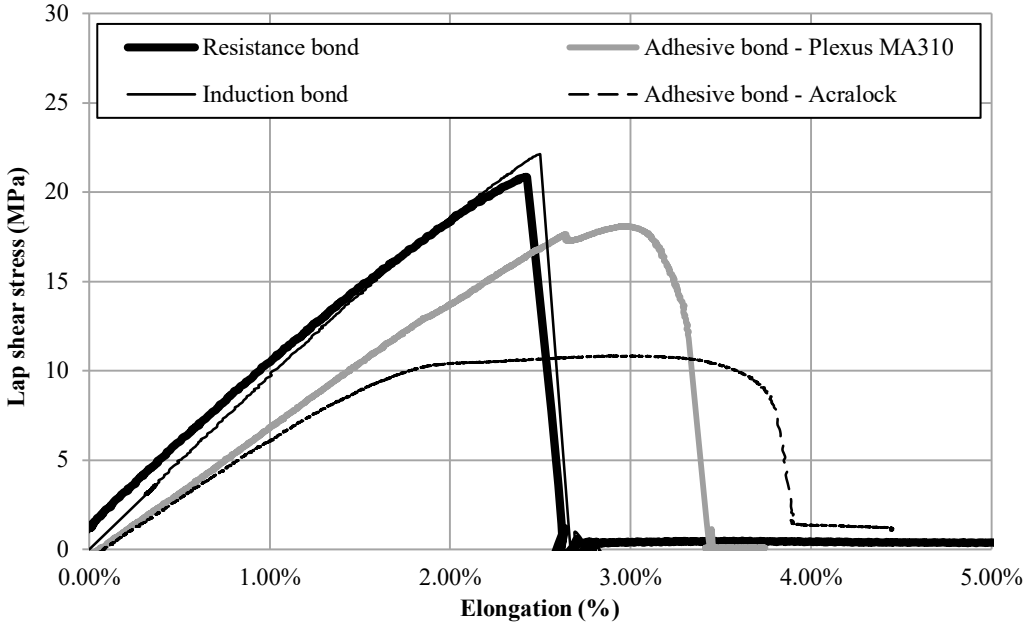

Figure 11 Elongation to failure as a function of lap-shear stress for various bonds.

As shown in Figure 11, although the fusion bonds had higher lap-shear strengths, the adhesive bonds were more ductile, showing higher elongation at failure. In a brittle failure mode, the bond can have high strength but the concentrated stress becomes critical and crack propagation along the interface occurs very fast, so the load-deflection curve drops suddenly at the maximum failure load [44]. Petterson [30] showed that a high failure strength and high fracture toughness will yield a robust and strong joint design, but that a lower failure strength can be compensated for if a more ductile adhesive is used. This is attributed to the stresses redistributing better in a ductile adhesive, thereby improving utilization of the entire bond area. DNV-GL [39] categorizes adhesives as either rigid or flexible, where rigid adhesives have high strength with high stiffness (one typical example is high-performance epoxy adhesives) and flexible adhesives have low strength, low stiffness, and high strain to failure (one typical example is polyurethane adhesives). Based on the type of adhesive, the DNV-GL guidelines specify the allowable lap-shear strength values. For rigid adhesives, DNV-GL requires 12-MPa tensile lap-shear strength after 24 ± 1 h curing at 23°C and storage at 50% relative humidity, whereas for flexible adhesives the tensile lap-shear strength has to be greater than 2 MPa for approval according to class A. In the case of the adhesives and fusion bonds presented here, both types of bonds meet the minimum requirements set by DNV-GL, independent of the type of failure. The fact that the lap-shear strength is significantly higher for the fusion bonds suggests that these bonds could survive higher loading once deployed on a wind turbine blade, which might outweigh the ability of the more ductile adhesives to distribute the loads better. Furthermore, the increased toughness of these joints might help mitigate erosion. Future work will include fracture toughness characterization to further explore the performance of these new fusion-welded bonds.

Pursuant to the DOE Public Access Plan, this document represents the authors' peer-reviewed, accepted manuscript. The published version of the article is available from the relevant publisher.

3.2 Fatigue results

With the high level of cyclic loading that wind turbine blades are exposed to, the fatigue performance of materials used in the blades is critical. To characterize the fatigue strength of the thermoplastic composite bonds, resistance-welded lap-shear specimens, as well as bonds made with the Plexus MA310 (which was found to have the highest static lap-shear strength), were characterized in fatigue using the 100-kN MTS load frame. Because of the limitations and sensitivity of the coil placement for induction welding, as well as the temperature nonuniformity in the heating element, resistance welding is thought to be a better solution for fusion joining of full-scale wind turbine blades. Therefore, the authors chose to focus on resistance welding for the fatigue testing. The fatigue limit, defined as the shear stress at which no failure occurs after 10 million cycles, was found to be approximately 5 MPa for the fusion-welded bonds and 3 MPa for the adhesive bonds. The fatigue life versus applied stress (S-N curve) is shown in Figure 12.

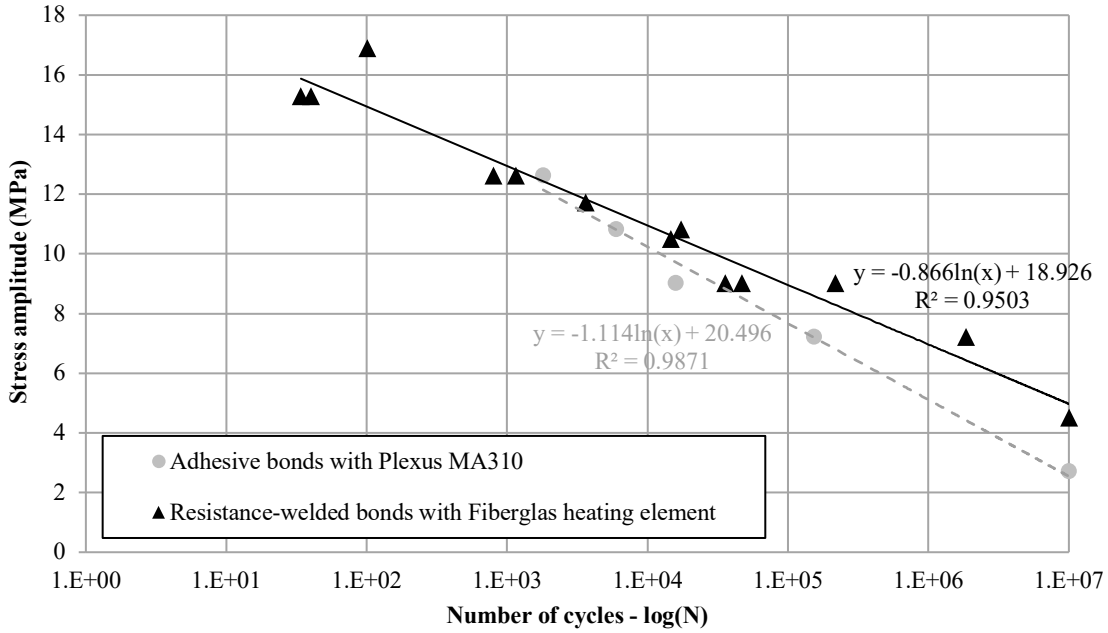

Figure 12 S-N curve for fusion-welded and adhesively bonded lap-shear specimens.

At a lower number of cycles, the adhesive and resistance-welded bonds had a similar fatigue life. However, at a higher number of cycles the welded bonds had a higher fatigue life than the adhesive bonds. Although the adhesive samples did meet the 1 MPa for 1 million cycles required by DNV-GL [45], this finding suggests that fusion-welded bonds have the potential to last longer in the field under the cyclic loading of a wind turbine blade. At the lower cycle and higher stress loading, there was more scatter in the resistance-welded bond strengths, which is attributed to more catastrophic and brittle failures occurring, compared to the high cycle fatigue results when the coupons eventually fail because of an accumulation of small localized failures.

Pursuant to the DOE Public Access Plan, this document represents the authors' peer-reviewed, accepted manuscript. The published version of the article is available from the relevant publisher.

These results are similar to those presented by Dube [35], who showed a logarithmic trend between applied load and cycles to failure with a fatigue limit of about 20% of the static lap-shear strength for resistance-welded bonds.

4 Future challenges

The lap-shear results had some scatter, as shown by the error bars in Figure 6, because of the challenges discussed earlier. However, beyond sizing incompatibility and incomplete infusion issues, there were additional process challenges and uncertainty that were not included in the results presented here. First, the surface quality of the adherends played an important role in the bond quality. In some cases, the panels used to make the adherends had resin-starved areas on the surface that resulted in the bonds failing at the glass fibers on the surface of the adherend. This was addressed by improving the panel manufacturing process to ensure high-quality panels. Additionally, it was challenging to locate the thermocouples in the bond area repeatedly to make sure that the temperatures achieved from bond to bond were the same. This is expected to be less of an issue for heating elements that have improved temperature uniformity, which is a focus of future work. Finally, we experimented in achieving an electrically consistent connection between the power supply and the heating element. Distribution of current flow across the heating element is thought to vary based on the distribution of clamping pressure, cleanliness of the copper connecting elements, and distribution of the fibers relative to one another. A new copper busbar is being developed that will be stiffer to better distribute clamping loads and also provide ridged features to ensure adequate electrical connection to the heating elements.

The next stages of this work focus on scaling up fusion joining for large wind turbine blades. One of the most important considerations for scaling up resistance welding for wind turbine blades is the bond gap tolerances that are taken up by adhesives. Currently, wind turbine blades bonded with an adhesive have a bond gap that can range from 1 to 20 mm. For successful joining, the adjacent components in a bond will have to be in contact, requiring tighter tolerances. However, decreasing manufacturing tolerances will be expensive, therefore, future work will investigate new blade joint designs to enable fusion joining with existing tolerances or welding method modifications that enable adequate contact with existing blade tolerances. Further, with the addition of conductive heating elements in the bond lines, lightning protection is a critical consideration for fusion-joined wind turbine blades, and appropriate lightning protection systems will have to be designed and verified. Furthermore, differences in the rate of thermal expansion between the heating element and the fiberglass components could be an issue in field operation as well as during manufacturing and will have to be carefully considered. Finally, methods will have to be explored to enable the pressure required during fusion joining for a full-scale blade.

Pursuant to the DOE Public Access Plan, this document represents the authors' peer-reviewed, accepted manuscript. The published version of the article is available from the relevant publisher.

5 Conclusions

This work presents one of the first investigations into advanced joining methods for wind turbine blades using infusible thermoplastic resins. Thermoplastic composite bonds made with adhesives commonly used for wind turbine blade manufacturing were compared to resistance- and induction-welded bonds. The fusion-welded thermoplastic composite bonds had higher static and fatigue lap-shear strengths than commonly used wind turbine blade adhesives. Various failure modes were observed for the fusion-welded bonds and scanning electron microscopy was used to identify improvements in the bonding process that are needed to increase bond strengths. Future work will be directed at improving the carbon-fiber heating element infusion and the resin to carbon-fiber adhesion. Future work will also include a more in-depth evaluation of the fracture mechanics of fusion-welded bonds using other characterization methods such as peel tests so that additional failure modes can be explored.

Based on the power requirements and heating time for lap-shear specimens and compared to the current time to apply adhesives during blade manufacturing, it is expected that fusion joining will decrease in-mold cycles times at wind turbine blade manufacturing facilities. The outcomes of this work demonstrate that fusion joining has the potential to result in stronger bonds with decreased manufacturing times, and hence decreased blade costs. Resistance welding has been identified as the best path forward for controlled, low-cost fusion joining for wind turbine blade components. Future work is focused on scaling up to a subcomponent blade scale and verifying larger bond areas through structural characterization. This will include investigating joining method compatibility with blade design requirements and manufacturing processes.

Acknowledgments

Thank you to Bobby To at the National Renewable Energy Laboratory for SEM imaging. Thank you to Jessica Lavorata and Ryan Clarke, interns with the Institute for Advanced Composites Manufacturing Innovation at the National Renewable Energy Laboratory, for their background research on fusion joining. Thank you also to Nathan Bachman at Arkema Inc and Neil Smith at Composite One for their support and for supplying materials for this research. This work was authored by the National Renewable Energy Laboratory (NREL), operated by Alliance for Sustainable Energy, LLC, for the U.S. Department of Energy (DOE) under Contract No. DE-AC36-08GO28308. This work was supported by the Laboratory Directed Research and Development (LDRD) Program at NREL. The views expressed in the article do not necessarily represent the views of the DOE or the U.S. Government. The U.S. Government retains and the publisher, by accepting the article for publication, acknowledges that the U.S. Government retains a nonexclusive, paid-up, irrevocable, worldwide license to publish or reproduce the published form of this work, or allow others to do so, for U.S. Government purposes.

Pursuant to the DOE Public Access Plan, this document represents the authors' peer-reviewed, accepted manuscript. The published version of the article is available from the relevant publisher.

References

1. Y. Zuo, J. Montesano, and C. V. Singh, "Assessing progressive failure in long wind turbine blades under quasi-static and cyclic loads". *Renewable Energy*, 2018. **119**: p. 754-766.
2. Y. Hua, A. R. M. Kasavajhala, and L. Gu, "Elastic–plastic analysis and strength evaluation of adhesive joints in wind turbine blades". *Composites Part B: Engineering*, 2013. **44** (1): p. 650-656.
3. J. B. Jørgensen, B. F. Sørensen, and C. Kildegaard, "Tunneling cracks in full scale wind turbine blade joints". *Engineering Fracture Mechanics*, 2018. **189**: p. 361-376.
4. R. Yang, Y. He, and H. Zhang, "Progress and trends in nondestructive testing and evaluation for wind turbine composite blade". *Renewable and Sustainable Energy Reviews*, 2016. **60**: p. 1225-1250.
5. F. M. Jensen, B. G. Falzon, J. Ankersen, and H. Stang, "Structural testing and numerical simulation of a 34m composite wind turbine blade". *Composite Structures*, 2006. **76** (1-2): p. 52-61.
6. L. C. T. Overgaard, E. Lund, and O. T. Thomsen, "Structural collapse of a wind turbine blade. Part A: Static test and equivalent single layered models". *Composites Part A: Applied Science and Manufacturing*, 2010. **41** (2): p. 257-270.
7. L. C. T. Overgaard and E. Lund, "Structural collapse of a wind turbine blade. Part B: Progressive interlaminar failure models". *Composites Part A: Applied Science and Manufacturing*, 2010. **41** (2): p. 271-283.
8. J. Yang, C. Peng, J. Xiao, J. Zeng, S. Xing, J. Jin, and H. Deng, "Structural investigation of composite wind turbine blade considering structural collapse in full-scale static tests". *Composite Structures*, 2013. **97**: p. 15-29.
9. D. S. Zarouchas, A. A. Makris, F. Sayer, D. Van Hemelrijck, and A. M. Van Wingerde, "Investigations on the mechanical behavior of a wind rotor blade subcomponent". *Composites Part B: Engineering*, 2012. **43** (2): p. 647-654.
10. B. L. Ennis and J. A. Paquette, *NRT Rotor Structural/Aeroelastic Analysis for the Preliminary Design Review*. 2015, Sandia National Laboratories.
11. IACMI. "The Composites Institute Facilitates Thermoplastic Composite Development for Wind Turbine Blades through Innovative Project". [2017; Available from: http://iacmi.org/2017/01/17/iacmi-composites-institute-facilitates-thermoplastic-composite-development-wind-turbine-blades-innovative-project/.
12. D. S. Cousins, Y. Suzukia, R. E. Murray, J. R. Samaniuk, and A. P. Stebner, "Recycling glass fiber thermoplastic composites from wind turbine blades". *Journal of Cleaner Production*, 2018. **Submission number JCLEPRO-D-18-07661**: p.
13. H. E. N. Bersee and S. D. Noi. "Fast processing and material challenges". In *Wind Turbine Blade Manufacture*. 2016. Düsseldorf, Germany.
14. R. E. Murray, S. Jenne, D. Snowberg, D. Berry, and D. Cousins, "Techno-Economic Analysis of a Megawatt-Scale Thermoplastic Resin Wind Turbine Blade". *Renewable Energy*, 2018. **Available online 11 July 2018, In Press, Accepted Manuscript**: p.
15. K. Ramirez-Tejeda, D. A. Turcotte, and S. Pike, "Unsustainable Wind Turbine Blade Disposal Practices in the United States". *New Solut*, 2017. **26** (4): p. 581-598.
16. R. Wiser and M. Bolinger, *2015 Wind Technologies Market Report*. 2015, U.S. Department of Energy.
17. T. J. Ahmed, D. Stavrov, H. E. N. Bersee, and A. Beukers, "Induction welding of thermoplastic composites—an overview". *Composites Part A: Applied Science and Manufacturing*, 2006. **37** (10): p. 1638-1651.
18. Personal Communication S. Nolet, *TPI Composites: Manufacturing wind turbine blade specifications* S. Jenne, D. Berry, and D. Snowberg, 2017.
19. P. Gouin O'Shaughnessey, M. Dubé, and I. Fernandez Villegas, "Modeling and experimental investigation of induction welding of thermoplastic composites and comparison with other welding processes". *Journal of Composite Materials*, 2016. **50** (21): p. 2895-2910.
20. C. Ageorges, L. Ye, and M. Hou, "Experimental investigation of the resistance welding for thermoplastic-matrix composites. Part I: heating element and heat transfer". *Composites Science and Technology*, 2000. **60**: p. 1027-1039.
21. D. Stavrov and H. E. N. Bersee, "Resistance welding of thermoplastic composites-an overview". *Composites Part A: Applied Science and Manufacturing*, 2005. **36** (1): p. 39-54.
22. M. Hou, M. Yang, A. Beehag, Y.-W. Mai, and L. Ye, "Resistance welding of carbon fibre reinforced thermoplastic composite using alternative heating element". *Composite Structures*, 1999. **47** (1-4): p. 667-672.
23. T. Bayerl, M. Duhovic, P. Mitschang, and D. Bhattacharyya, "The heating of polymer composites by electromagnetic induction – A review". *Composites Part A: Applied Science and Manufacturing*, 2014. **57**: p. 27-40.
24. M. Matsen, *Induction Consolidation/Molding of Thermoplastic Composites Using Smart Susceptors*. 2012, The Boeing Company.
25. M. J. Troughton, *Handbook of plastics joining : a practical guide* Second ed. 2008: William Andrew Inc.
26. A. Yousefpour, M. Hojjati, and J.-P. Immarigeon, "Fusion Bonding/Welding of Thermoplastic Composites". *Journal of Thermoplastic Composite Materials*, 2016. **17** (4): p. 303-341.
27. H. SHI, "Resistance welding of thermoplastic composites Process and performance". 2014, Delft University of Technology
28. F. Aerostructures, *New evolution: Progress in thermoplastic composites*.
29. W. Suwanwatana, S. Yarlagadda, and J. W. Gillespie, "Influence of particle size on hysteresis heating behavior of nickel particulate polymer films". *Composites Science and Technology*, 2006. **66** (15): p. 2825-2836.
30. J. PETTERSSON, "Analysis and Design of an Adhesive Joint in Wind Turbine Blades", in *Structural Mechanics*. 2016, Lund University
31. Y. M. Ji and K. S. Han, "Fracture mechanics approach for failure of adhesive joints in wind turbine blades". *Renewable Energy*, 2014. **65**: p. 23-28.
32. F. Sayer, A. Antoniou, and A. van Wingerde, "Investigation of structural bond lines in wind turbine blades by sub-component tests". *International Journal of Adhesion and Adhesives*, 2012. **37**: p. 129-135.
33. W. R. Broughton, R. D. Mera, and G. Hinopoulos, *Cyclic Fatigue Testing of Adhesive Joints Test Method Assessment*, in *Project PAJ3 - Combined Cyclic Loading and Hostile Environments 1996-1999*, NPL, Editors. 1999.
34. W. Suwanwatana, S. Yarlagadda, and J. Gillespiejr, "Hysteresis heating based induction bonding of thermoplastic composites". *Composites Science and Technology*, 2006. **66** (11-12): p. 1713-1723.
35. M. Dubé, A. Chazerain, P. Hubert, A. Yousefpour, and H. E. N. Bersee, "Characterization of resistance-welded thermoplastic composite double-lap joints under static and fatigue loading". *Journal of Thermoplastic Composite Materials*, 2013. **28** (6): p. 762-776.
36. L. Boriwal, R. M. Sarviya, and M. M. Mahapatra, "Failure modes of spot welds in quasi – static tensile – shear loading of coated steel sheets". *Materials Today: Proceedings*, 2017. **4** (2): p. 3672-3677.
37. Acralock, *Acralock SA10-60 Technical Data Sheet*. 2016.
38. Plexus, *Plexus MA310 Technical Data Sheet*. 2014.
39. DNV-GL, *Adhesive systems*, in *CLASS PROGRAMME Type approval*. 2016.
40. J. L. Thomason, C. C. Kao, J. Ure, and L. Yang, "The strength of glass fibre reinforcement after exposure to elevated composite processing temperatures". *Journal of Materials Science*, 2013. **49** (1): p. 153-162.

Pursuant to the DOE Public Access Plan, this document represents the authors' peer-reviewed, accepted manuscript. The published version of the article is available from the relevant publisher.

41. S. Feih, K. Manatpon, Z. Mathys, A. G. Gibson, and A. P. Mouritz, "Strength degradation of glass and carbon fibres at high temperature". *Journal of Materials Science*, 2009. **44** (2): p. 392-400.
42. P. G. Jenkins, L. Yanga, J. J. Liggatb, and J. L. Thomasona, *Investigation of the strength loss of glass fibre after thermal conditioning*. 2014, University of Strathclyde.
43. Personal Communication N. Bachman, *Suitable for Glass-Reinforced Structural Parts*, R. Murray, 2018: Arkema Inc.
44. S. Sihn, Y. Miyano, and S. W. Tsai, *Time- and Temperature-Dependent Failures of a Bonded Joint* 1997, National Renewable Energy Laboratory and Stanford University
45. DNV-GL, *Rotor blades for wind turbines*. 2015.

Pursuant to the DOE Public Access Plan, this document represents the authors' peer-reviewed, accepted manuscript. The published version of the article is available from the relevant publisher.